International Journal of Thermophysics, Vol. 21, No. 4, 2000

Evaluation of Hemispherical Total Emissivity for Thermal Radiation Calorimetry

H. Tanaka,[1,2] S. Sawai,[1] K. Morimoto,[1] and K. Hisano[1]

Received November 23, 1999

An attempt to derive the hemispherical total emissivity from the normal emission spectrum is proposed for Vycor and fused silica glasses. The normal emission spectrum from a clear surface has been measured at steady state in the temperature range from 400 to 750 K. The sample is heated on one metal-backed face by thermal radiation from a heater. Temperatures inside the sample were monitored by thermocouples at two points near the surfaces. Evaluation of the hemispherical total emissivity from the normal emission spectrum is determined by means of Kramers–Krönig analysis and virtual mode equations. Assuming a linear temperature distribution within the sample, the thermal conductivities of silicate glasses were obtained at elevated temperatures. The results are comparable with those obtained by previous investigators. The effect of radiation heat transfer in a sample is also discussed.

KEY WORDS: calorimetry; emittance; fused silica; hemispherical total emissivity; refractive index; spectral emissivity; thermal conductivity; virtual mode; Vycor glass.

1. INTRODUCTION

Measurements of thermophysical properties under both steady- and quasi-steady-state conditions by means of thermal radiation calorimetry (TRAC) have been performed for thermal insulating materials [1, 2]. In this technique, both surfaces of a disk-shaped sample are blackened with a material whose surface emissivity is known. If we can estimate the value of the hemispherical total emissivity from the emission spectrum at various temperatures, the blackening is no longer necessary in order to obtain the

[1] Department of Mathematics and Physics, National Defense Academy, Yokosuka 239-8686, Japan.

[2] To whom correspondence should be addressed.

0195-928X/00/0700-0927$18.00/0

thermal conductivity by TRAC. A silicate glass has a high emissivity and a low thermal conductivity [3–5] and is not transparent in the far infrared region. These characteristics are suitable for the infrared experiment and analysis to obtain the emissivity and for the detection of a temperature gradient in a disk shaped sample to evaluate the thermal conductivity.

The hemispherical total emissivity of a material surface is generally obtained from the hemispherical emission spectrum and the spectral distribution function of blackbody radiation for the sample temperature. It is necessary to derive the frequency (or wave number) dependence of the real and imaginary parts of the refractive index (or dielectric constant) of a sample to obtain the hemispherical emission spectrum [6]. In this paper, an attempt to derive the hemispherical total emissivity from the normal emission spectrum is performed for Vycor and fused silica glasses. The hemispherical total emissivities are obtained in the temperature range between 400 and 750 K. The thermal conductivities of these samples are obtained by TRAC at steady state after the spectral analysis. The errors caused by radiation heat transfer in a semitransparent sample are estimated.

2. THEORETICAL FORMULATION

The theory of the present calorimeter has been described in detail in a previous paper [1]. The major difference is that in this study one surface of the sample is not blackened and is kept clean as polished for a spectral emissivity measurement. We consider a one-dimensional system in which a disk-shaped sample is heated on one face by radiation from a flat heater set in a plane parallel to the sample in a vacuum chamber at room temperature. Assuming the temperature gradient within the sample is linear for a steady state, the following equation is derived from the boundary condition at the back surface of the sample facing a spectrometer:

$$\lambda \frac{T_d - T_0}{d} = \varepsilon(I_0 - I_r) \tag{1}$$

where λ and d are the thermal conductivity and the sample thickness, respectively. T_0 and T_d are the temperatures of the surfaces facing a spectrometer and the heater, respectively. The radiant power I emitted by a perfect absorber at temperature T is given by $I = \sigma T^4$, where σ is the Stefan–Boltzmann constant. The subscripts 0 and r on the right side of Eq. (1) refer to T_0 and room temperature, respectively. ε is the hemispherical total emissivity of the sample surface. In Eq. (1), the effects of absorption-emission and scattering of radiation heat flux transferred in a sample are

ignored. ε is obtained from the hemispherical spectral emissivity ε_ν. That is,

$$\varepsilon = \frac{\int_0^\infty \varepsilon_\nu W(\nu, T)\, d\nu}{\int_0^\infty W(\nu, T)\, d\nu} \tag{2}$$

where $W(\nu, T)$ is Planck's emissive power at frequency ν. ε_ν is calculated from the following relation:

$$\varepsilon_\nu = 2 \int_0^{\pi/2} \varepsilon(\nu, \theta) \sin\theta \cos\theta\, d\theta \tag{3}$$

where $\varepsilon(\nu, \theta)$ is the directional emission spectrum and θ is the angle from the normal to the sample surface. In Eq. (3), we assumed the azimuthal directional emissivity is homogeneous.

Optical properties of an ionic crystal slab have been discussed in detail in terms of virtual-mode equations by Fuchs et al. [6]. They have shown explicitly the relation between the optical properties and the dielectric function $\xi(\nu)$. For the case of an ionic slab on a conducting substrate, the characteristic functions L_p and L_s, which determine the optical properties for p- and s-polarization, are given by

$$L_p = 1 - i \frac{\beta}{\beta_0 n_c^2(\nu)} \tan(\beta d) \tag{4}$$

$$L_s = 1 + i \frac{\beta}{\beta_0} \cot(\beta d) \tag{5}$$

where $\beta = 2\pi\nu \{ n_c^2(\nu) - \sin^2\theta \}^{1/2}$ and $\beta_0 = 2\pi\nu \cos\theta$. $n_c(\nu)$ is the complex refractive index given by $\xi(\nu) = n_c^2(\nu)$. In this situation, the directional emission spectra $\varepsilon_p(\nu, \theta)$ for p-polarization and $\varepsilon_s(\nu, \theta)$ for s-polarization can be written

$$\varepsilon_p(\nu, \theta) = 1 - \left| \frac{2 - L_p}{L_p} \right|^2 \tag{6}$$

$$\varepsilon_s(\nu, \theta) = 1 - \left| \frac{2 - L_s}{L_s} \right|^2 \tag{7}$$

If the real and imaginary parts of the complex refractive index are $n(\nu)$ and $k(\nu)$, $n_c(\nu)$ is expressed as

$$n_c(\nu) = n(\nu) + ik(\nu) \tag{8}$$

Thus, we can calculate the emissivity from the virtual mode equations, knowing the real and imaginary parts of the complex refractive index at various frequencies. For unpolarized radiation, the emissivity $\varepsilon(\nu, \theta)$ becomes

$$\varepsilon(\nu, \theta) = \tfrac{1}{2}[\varepsilon_P(\nu, \theta) + \varepsilon_P(\nu, \theta)] \tag{9}$$

Kramers–Krönig analysis can be performed for the normal reflection spectra to obtain the complex refractive index at various frequencies. The reflection spectrum can be obtained from the measured emission spectrum based on Kirchhoff's law for thermal radiation [7, 8]. For the frequency range where the sample shows no transmission, it reduces to

$$R(\nu, 0) = 1 - \varepsilon(\nu, 0) \tag{10}$$

where $R(\nu, 0)$ and $\varepsilon(\nu, 0)$ are the normal reflection and emission spectra, respectively. In the high-frequency range where the transmission is observed, we cannot use Eq. (10). If we can estimate the dispersion relation in this region, we are able to calculate the reflectivity $R_c(\nu)$, since the normal incidence reflectivity for unpolarized light is generally given by

$$R_c(\nu) = \left| \frac{\sqrt{\xi(\nu)} - 1}{\sqrt{\xi(\nu)} + 1} \right|^2 \tag{11}$$

For an ionic material, the transmission occurs usually above the highest longitudinal optical (LO) mode frequency ν_L in the slab. It is well known that we observe neither reflection nor transmission at a frequency ν_R slightly above ν_L when the sample is bulk material [9]. In other words, the emissivity becomes 100% around ν_R. On the other hand, $\sqrt{\xi(\nu)}$ at a very high frequency can be regarded as the refractive index for visible light n_∞ [4]. Thus, Eq. (11) for $\nu \geqslant \nu_R$ is considered to be a smooth function starting from a minimum close to zero around ν_R and approaching an asymptotic line (about 0.04) given by $n_\infty = 1.5$ at a high frequency for silicate glass [10]. In this study a dielectric function with a harmonic oscillator form is applied to estimate the reflectance in this high-frequency region for simplicity. That is,

$$\xi(\nu) = n_\infty^2(\nu_L^2 - \nu^2)/(\nu_T^2 - \nu^2) \tag{12}$$

where ν_T is the frequency of the transverse optic (TO) mode responsible for the highest LO mode.

After estimating the refractive index from the reflectivity $R(\nu, 0)$ for $\nu \leqslant \nu_R$ and $R_c(\nu)$ for $\nu \geqslant \nu_R$ by Kramers–Krönig analysis, the imaginary part $k(\nu)$ for $\nu \geqslant \nu_R$ is obtained as follows. Since the dielectric function of

a harmonic oscillator is real, we cannot obtain the imaginary part of the refractive index from Eq. (12) for $\nu \geqslant \nu_R$. When transmission is observed in a sample with low reflectivity as in silicate glasses, the effective transmittance T^* is given by

$$T^* = \exp[-4\pi\nu k(\nu)\, L] \tag{13}$$

where $4\pi\nu k(\nu)$ and L are the absorption coefficient and the optical path length, respectively. For an ionic slab on a conducting substrate, L should be read as $2d$, because the coated metal works as a mirror. According to Kirchhoff's law for a semitransparent material, on the other hand, T^* should satisfy the following relation:

$$T^* = 1 - R_c(\nu) - \varepsilon(\nu, 0) \tag{14}$$

Using Eqs. (13) and (14), we can estimate the imaginary part of the complex refractive index in the high-frequency region where the sample may be transparent.

3. EXPERIMENT

A schematic of TRAC for a spectral measurement is illustrated in Fig. 1. The apparatus components are enclosed inside a water-cooled vacuum chamber (not shown). Disk-shaped samples of Vycor and fused silica with a thickness of 5 mm were examined. Their diameters are 25 mm for Vycor and 30 mm for fused silica. All surfaces of the samples are

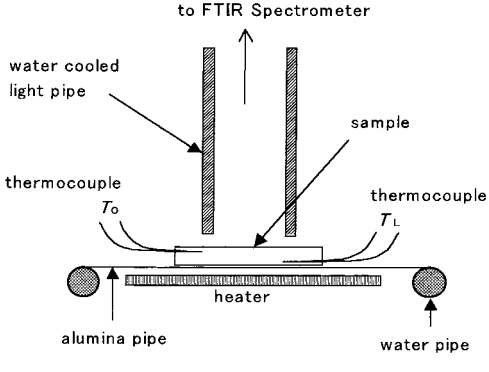

Fig. 1. Schematic configuration of TRAC for a spectral measurement. The dimensions of the heater and the light pipe are 5 cm square and 20 mm in diameter, respectively.

polished to optical grade. The bottom and side surfaces of the sample were coated with a metal by vacuum deposition. Copper was used as a coating material, since copper shows a high reflectivity comparable to that of gold in the infrared region. The thickness of the copper film was about 0.1 to 0.2 μm, which was stable for several heating cycles between room temperature and 800 K. Such a metal coating was applied to prevent radiation heat transfer through the surfaces except for the top surface facing a spectrometer as shown schematically in Fig. 1.

Unlike previous TRAC, only one face of the sample facing a flat heater, the bottom face of the sample, is blackened after the metal coating is applied. This blackening is done with colloidal graphite because the sample has to be heated from only one surface which absorbs the radiation from the heater. The copper coating was also stable for the graphite coating. The metal coat prior to blackening ensures that the sample is actually heated by conduction because the system, which consists of a coated metal and a blackening material, works as a conductive heater attached to the sample. The side surface of the sample is kept clean as copper is deposited. The remaining surface of the sample facing a spectrometer is kept clean as polished.

The normal emission spectrum from the clear top surface has been measured at steady state in the temperature range from 400 to 750 K. The temperature inside the sample was monitored at two points by the use of thermocouples mounted near the surfaces as described previously [2]. The surface temperatures are derived assuming a linear temperature distribution within the sample. A Jasco 610 FTIR spectrometer with a CsI beam splitter and DLTGS detector is employed for the spectrum measurement at 16-cm^{-1} resolution.

4. RESULTS AND DISCUSSION

The open circles in Fig. 2 show the normal emission spectrum $\varepsilon(\nu, 0)$ of Vycor glass measured at a surface temperature $T_0 = 585$ K. This spectrum contains a small amount of extra emission above ν_R because of nonhomogeneous temperature distribution within the sample. The filled circles (in Fig. 2) show the hemispherical emission spectrum ε_ν calculated from Eqs. (3) and (9). The dashed line indicates the wave-number dependence of black body radiation intensity normalized with the intensity at the peak frequency ν_P. From Fig. 2 ν_R is read as about 1350 cm^{-1}. The refractive index obtained before virtual mode analysis is shown in Fig. 3. In the Kramers–Krönig analysis, we assumed the values of n_∞, ν_L, and ν_T to be 1.5, 1190 cm^{-1}, and 1040 cm^{-1}, respectively. These values were estimated from a preliminary analysis of the reflection spectra measured at room

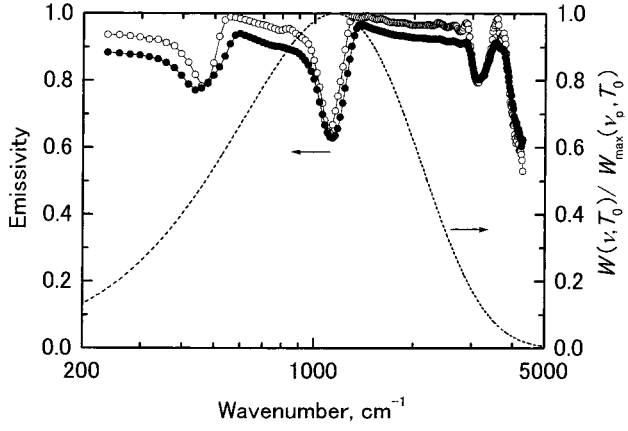

Fig. 2. Emission spectra of Vycor glass measured at $T_0 = 585$ K and wave-number dependence of blackbody radiation intensity. (○) Normal emission spectrum; (●) hemispherical emission spectrum; (----) blackbody.

temperature. Figure 4 shows the total emissivities at various temperatures. The open and filled circles indicate the *normal* total emissivity and the *hemispherical* total emissivity calculated from Eq. (2). Figure 5 shows the temperature difference between the two faces assuming the distribution to be linear in the sample. Figures 6 to 9 show the results obtained for fused silica. The spectra and refractive index shown in Figs. 6 and 7 are obtained

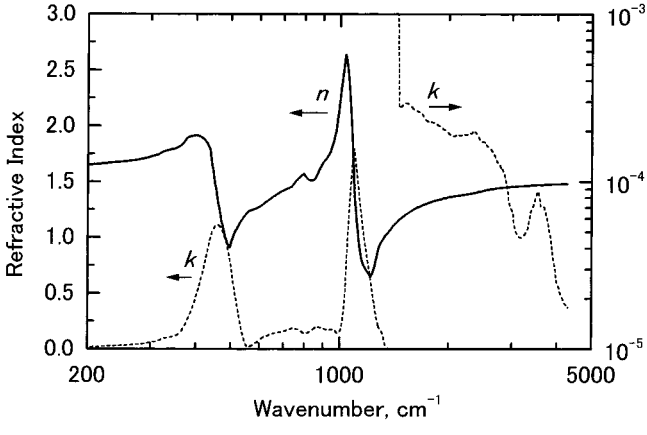

Fig. 3. Refractive index of Vycor glass at $T_0 = 585$ K. Solid line, real part; dashed line, imaginary part.

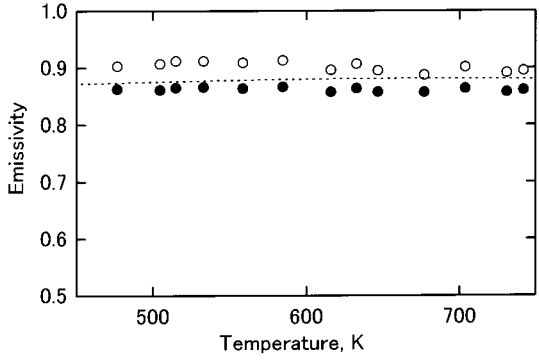

Fig. 4. Emissivity of Vycor glass. (○) Normal total emissivity; (●) hemispherical total emissivity; (----) normal total emissivity from the data of Ref. 3.

at $T_0 = 590$ K. We assumed the values of n_∞, ν_L, and ν_T to be 1.5, 1195 cm^{-1}, and 1045 cm^{-1}, respectively. The ν_R for fused silica is also about 1350 cm^{-1} as seen in Fig. 6.

It should be noted that the values of ν_L and ν_T were not sensitive to the present results plotted in Figs. 4 and 8. Even if we changed these values by 10%, the resulting deviations in the emissivity were less than 1%. However, the values of n_∞, ν_L, and ν_T mentioned above were selected as Eq. (11) is closely connected to Eq. (10). In other words, we can obtain good continuity in the reflection spectrum and refractive index around ν_R

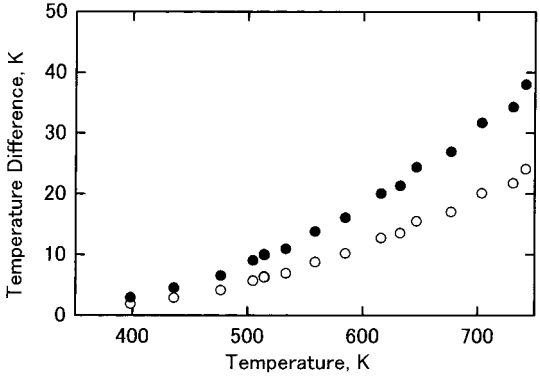

Fig. 5. Temperature difference between surfaces (●) and between thermocouples (○) for Vycor glass with a thickness of 5.01 mm. The thermocouple separation is 3.17 ± 0.05 mm.

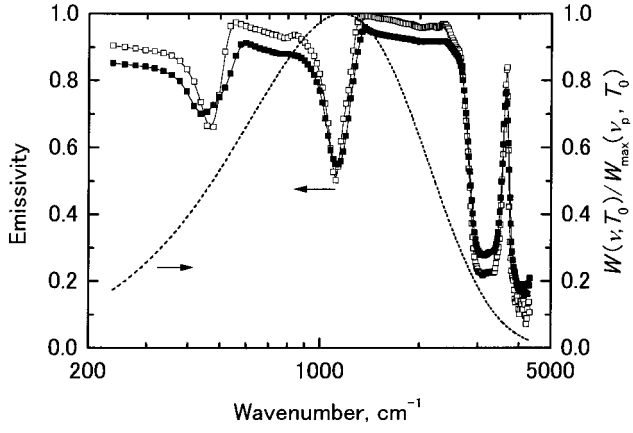

Fig. 6. Emission spectra of fused silica measured at $T_0 = 590$ K and wave-number dependence of blackbody radiation intensity. (□) Normal emission spectrum; (■) hemispherical emission spectrum; (– – – –) blackbody.

by adjusting the mode frequencies. The value of $n_\infty = 1.5$ corresponds to the refractive index of fused silica for 265-nm light [10]. The optic mode frequencies are about 3% different from those of crystalline quartz measured by Raman scattering [11], as is usual in silicate glasses. We have tried to analyze the spectra employing a damped harmonic oscillator form for the dielectric function. However, the fitting process was more

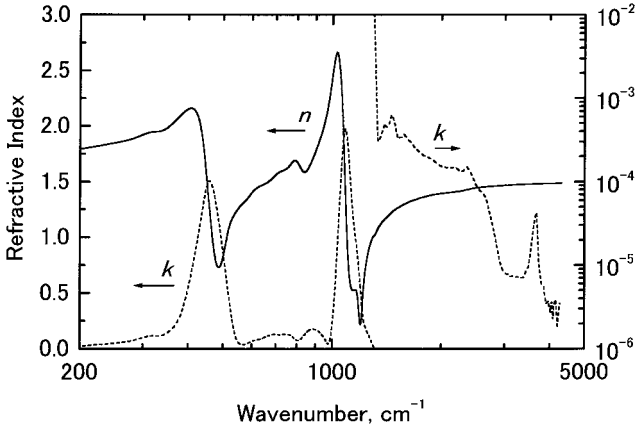

Fig. 7. Refractive index of fused silica at $T_0 = 590$ K. Solid line, real part; dashed line, imaginary part.

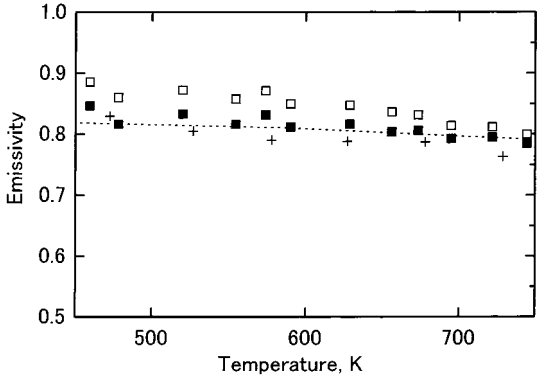

Fig. 8. Emissivity of fused silica. (□) Normal total emissivity; (■) hemispherical total emissivity; (– – – –) normal total emissivity from the data of Ref. 3; (+) normal total emissivity from Ref. 4.

complicated. The adjustment of the width of LO–TO splitting $(\nu_L - \nu_T)$ without increasing the number of parameters is convenient and seems to be allowed in the present case, since Eq. (11) is used only for the high-frequency range above ν_R. For the same reason, the effects of the damping factor on the dielectric function might not be as important as the TO–LO splitting.

The normal total emissivity obtained previously by a nonspectroscopic (direct) measurement of the thermal radiation from a 12.7-mm-thick sample

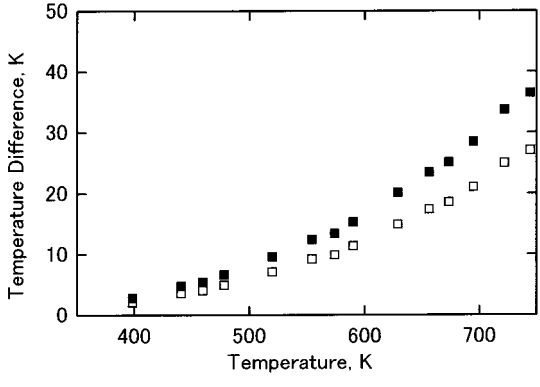

Fig. 9. Temperature difference between surfaces (■) and between thermocouples (□) for fused silica with a 5.03-mm thickness. The thermocouple separation is 3.73 ± 0.05 mm.

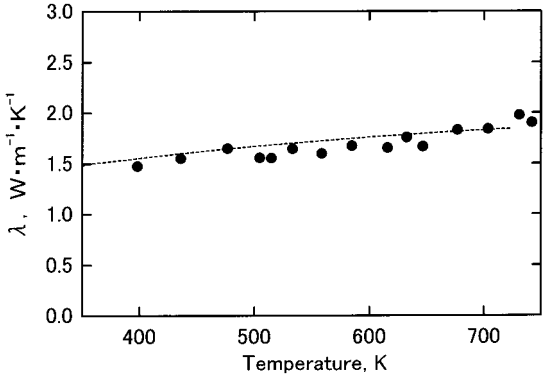

Fig. 10. Thermal conductivity of Vycor glass. (●) Present results; (–––) from the data of Ref. 12.

(in air) [3, 4] is also plotted in Figs. 4 and 8. Since the present samples are regarded as ionic slabs on a conducting material, their emissivities correspond to those for a thickness of 10 mm in free space [6]. The differences in the normal emissivity for the low-temperature region around 450 K are estimated to be about 3% for Vycor and 6% for fused silica, although the emissivity depends on the thickness of the sample. As far as we know, there are no experimental data for the total hemispherical emissivity by a spectroscopic study comparable with the present results. The next step is to evaluate the thermal conductivity by Eq. (1).

Figures 10 and 11 show the temperature dependences of the thermal conductivity of Vycor and fused silica, respectively. The filled circles and

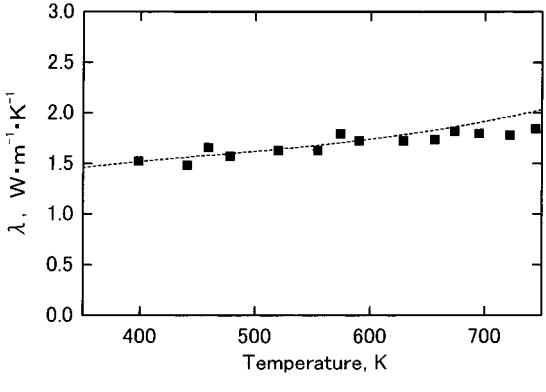

Fig. 11. Thermal conductivity of fused silica. (■) Present results; (––––) from the data of Ref. 5.

squares show the present results obtained from Eq. (1). The dashed lines are plotted after interpolation of the data from previous authors [5, 12]. As is easily seen, the results by spectral TRAC proposed here are comparable with those by other methods. From the point of view of Eq. (1), we can believe that the present procedure to derive the hemispherical total emissivity from the normal emission spectrum is reliable. If the hemispherical total emissivity were 3 or 6% lower than the present results, the values of the thermal conductivity would be lower by the same amount.

A nonhomogeneous temperature distribution within the sample caused by radiation heat transfer may become a source of error in the values of the thermal conductivity through ε. If scattering of radiation in a medium can be neglected, the error is estimated by analogy with the case of a gray gas [13]. Assuming that $T_d - T_0 \ll T_0$ and a linear temperature distribution in the slab, we can write the emissivity as

$$\varepsilon \approx \varepsilon_1 + \varepsilon_2(1+\delta) \tag{15}$$

where

$$\delta = \frac{4}{a_P d}\left(\frac{T_d - T_0}{T_0}\right)\tanh\left(\frac{-a_P d}{2}\right) \tag{16}$$

ε_1 and ε_2 are, respectively, the emissivities below and above ν_R:

$$\varepsilon_1 = \frac{\int_0^{\nu_R} \varepsilon_\nu W(\nu, T)\, d\nu}{\int_0^{\infty} W(\nu, T)\, d\nu} \tag{17}$$

$$\varepsilon_2(1+\delta) = \frac{\int_{\nu_R}^{\infty} \varepsilon_\nu W(\nu, T)\, d\nu}{\int_0^{\infty} W(\nu, T)\, d\nu} \tag{18}$$

a_P is the Planck's mean absorption coefficient [13] above ν_R given by

$$a_P = \frac{\int_{\nu_R}^{\infty} \alpha(\nu)\, W(\nu, T)\, d\nu}{\int_0^{\infty} W(\nu, T)\, d\nu} \tag{19}$$

where $\alpha(\nu) = 4\pi\nu k(\nu)$. For the case of large absorbance, Eq. (15) becomes $\varepsilon \approx \varepsilon_1 + \varepsilon_2$ since $\delta \approx 0$ for $a_P d \gg 1$. However, some errors must be contained in ε in the range where a_P is small. We have estimated the excess emissivity $\varepsilon_2\delta$ in Eq. (15). The values for the present silicate glass samples were less than 1.5% of the total emissivity around 400 K and 7% around 750 K.

From the point of view of Eqs. (15) and (16), the spectral TRAC method can be applied for materials with a high LO mode frequency (or v_R) and large absorption ($a_P d$) above v_R. In other words, it is preferable that the transmission may occur at a frequency higher than the peak of the blackbody radiation at the sample temperature. If these conditions can be satisfied, the effects of radiation heat transfer may still be small.

The deviation from the pure-conduction temperature distribution caused by radiation heat transfer may also become an error source in the determination of the thermal conductivity. The temperature distribution in a plane layer of a absorbing–emitting semitransparent solid has been investigated for various boundary conditions by Anderson et al. [14]. The results indicate that the deviation is approximately 5 K, at most, for a 12.7-mm-thick sample of fused quartz with a 200 K temperature difference at around 930 K. In the present case, the temperature difference is approximately 40 K for a thickness of 5 mm at around 750 K. Therefore, we can expect the deviation in the present samples to be less than 2 K at high temperature and the resulting error in the thermal conductivities less than 5%.

Although the thickness of the disk-shaped sample is preferably small, we need, at least, a 3-mm-thick sample in order to measure the temperature gradient in Eq. (1) using thermocouples [2]. The diameter of the sample available for spectral TRAC depends on the dimensions of the heater and the light pipe as illustrated in Fig. 1. In the present setup, it ranges from 25 to 30 mm.

4. CONCLUSION

Kramers–Krönig analysis and virtual mode equations have been applied to obtain the hemispherical total emissivity from the normal emission spectrum for a semitransparent sample. These results are employed to derive the values of thermal conductivity by TRAC for steady-state conditions. Comparing the current results for Vycor and fused silica with previous results [3–5, 12] at high temperatures, it is shown that the present method is reliable to determine the hemispherical total emissivity. The errors in both emissivity and temperature difference caused by the radiation heat transfer in the samples have also been discussed.

REFERENCES

1. K. Hisano, *Int. J. Thermophys.* **18**:535 (1997).
2. K. Hisano, S. Sawai, and K. Morimoto, *Int. J. Thermophys.* **20**:733 (1999).
3. O. H. Olson and J. C. Morris, *WADC Techn. Rep.* **56-222**(Pt III):1 (1960).

4. E. E. Anderson and J. Ozel, in *Heat Transfer*, U. Grigull, E. Hahne, K. Stephan, and J. Straub, eds. (7th Int. Heat Transfer Conf., München, 1982), Vol. 2, p. 457.
5. Y. S. Touloukian, R. W. Powell, C. Y. Ho, and P. G. Klemens, *Thermophysical Properties of Matter 2*, *Thermal Conductivity in Nonmetallic Solids* (Plenum, New York, 1972), p. 183.
6. R. Fuchs, K. L. Kliewer, and W. J. Pardee, *Phys. Rev.* **150**:589 (1966).
7. T. O. McMahon, *J. Opt. Soc. Am.* **40**:276 (1950).
8. K. Hisano, *J. Phys. Soc. Jpn.* **25**:1091 (1968).
9. T. Makino, I. Sakai, H. Kinoshita, and K. Kunitomo, *Trans. JSME* **50**:1045 (1984).
10. For example, J. H. Malitson, *J. Opt. Soc. Am.* **57**:674 (1967).
11. T. Sakudo, *Solid State Physics: Lattice Dynamics and Dielectric Phase Transitions* (Shokabo, Tokyo, 1993), p. 91.
12. Corning International Co. Ltd., private communication.
13. R. Siegel and J. R. Howell, *Thermal Radiation Heat Transfer* (Taylor and Francis, Washington, DC, 1992).
14. E. E. Anderson, R. Viskanta, and W. H. Stevenson, *J. Heat Transfer* **95**:179 (1973).